International Journal of Multiphase Flow 34 (2008) 1099–1107

Contents lists available at ScienceDirect

International Journal of Multiphase Flow

journal homepage: www.elsevier.com/locate/ijmulflow

SVR-based prediction of point gas hold-up for bubble column reactor through recurrence quantification analysis of LDA time-series

A.B. Gandhi [a], J.B. Joshi [a], A.A. Kulkarni [b], V.K. Jayaraman [b], B.D. Kulkarni [b,*]

[a] Institute of Chemical Technology, University of Mumbai, Matunga, Mumbai 400 019, India
[b] Chemical Engineering & Process, Development Division, National Chemical Laboratory, Pune 411008, India

ARTICLE INFO

Article history:
Received 27 December 2007
Received in revised form 15 July 2008
Available online 24 July 2008

Keywords:
Bubble column
LDA
Gas hold-up
Recurrence quantification analysis (RQA)
Support vector regression (SVR)

ABSTRACT

Recurrence quantification analysis (RQA) has emerged as a useful tool for detecting singularities in non-stationary time-series data. In this paper, we use RQA to analyze the velocity–time data acquired using laser doppler anemometry (LDA) signals in a bubble column reactor for Single point and Multipoint point spargers. The recurring dynamical states within the velocity–time-series occurring due to the bubble and the liquid passage at the point of measurement, are quantified by RQA features (namely % Recurrence, % Determinism, % Laminarity and Entropy), which in turn are regressed using support vector regression (SVR) to predict the point gas hold-up values. It has been shown that SVR-based model for the bubble column reactor can be potentially useful for online prediction and monitoring of the point gas hold-up for different sparging conditions.

1. Introduction

Bubble columns are very widely used in chemical process industry because of simple construction and ease of operation. In bubble columns, the gas phase is in the form of dispersed bubbles in a continuous liquid-phase. The gas hold-up directly decides the reactor volume depending upon the phase in which the reaction occurs. Indirectly, the gas hold-up profiles govern the liquid-phase flow pattern and hence the rates of mixing, heat transfer and mass transfer. Thus an adequate knowledge of gas hold-up and its profile is needed for modeling, design and scale-up of bubble column reactors. Therefore, it becomes essential to establish a model that can predict and monitor the point gas hold-up values on real-time basis at various axial and radial locations of the column reactor.

With the help of advanced experimental techniques, it is now possible to take time dependent measurements at various locations in the column. Analysis of such time-series data (velocity, pressure, capacitance, conductivity, etc.) is seen to yield more meaningful information about system characteristics on real-time basis. However, the measured signals generally show non-stationary characteristics as may be seen from their Fourier spectra which do not show consistency in frequency behavior over different time segments of data. This has thus involved the search for more powerful mathematical tools, which take into account the non-stationary features in the data and detect, analyze and cope with it. In this context, a recently introduced concept of recurrence quantification analysis (RQA), which relies on the presence of deterministic/recurring structures underlying the data, has been introduced into this paper (Ekmann et al., 1987; Castellini and Romanelli, 2004; Marwan, 2003; Webber and Zbilut, 2005; Zbilut et al., 2004). However, besides RQA, other non-linear time-series analysis techniques like chaos (Van den Bleek and Schouten, 1993; Letzel et al., 1997; Gandhi et al., 2007a) and wavelet (Kulkarni et al., 2001; Jade et al., 2006) have been used for the various studies pertaining to design of multiphase systems. Practically, the approach based on chaos is very similar to RQA. Both the approaches are based on the quantification of the phase-space plot constructed from the time-series. RQA is specifically based on the qualification as well the quantification of the number and duration of the recurrences, while, chaos analysis is based on the quantification of the extent of non-linearity (Lyapunov exponent and Kolmogorov entropy) of a non-linear dynamical system. Moreover, the main advantage of the RQA is that it provides useful information even for a short time-series. On the other hand wavelet transform (WT) is an appropriate mathematical function (based on wavelets) used to divide a given function or continuous-time signal into different frequency components and study each component with a resolution that matches its scale. Using a variable-size window in a time–frequency plane, WT provides an efficient approach by which both time and frequency resolutions are adjusted in an adaptive fashion. It uses a window that narrows when focusing on small-scale or high-frequency features of the signal and widens on large-scale or low-frequency features, analogous to a zoom lens. Thus, WT is

* Corresponding author. Tel.: +91 20 5893095; fax: +91 20 5893041.
E-mail address: bdk@ems.ncl.res.in (B.D. Kulkarni).

0301-9322/$ - see front matter © 2008 Elsevier Ltd. All rights reserved.
doi:10.1016/j.ijmultiphaseflow.2008.07.001

also known also as a mathematical microscope. Very recently both wavelet transformation and RQA have been employed by Sen et al. (2008) for analysis of cycle-to-cycle pressure oscillations in a diesel engine. The study found that the performance of both methodologies were similar. It can be observed that RQA requires the original time-series to be reconstructed by suitably choosing the attractor dimension and time delay, whereas we can directly transform the original time-series into frequency domain by wavelets. However, it can be observed that RQA provides a very small number of most informative features whereas wavelet transformation provides a large number of wavelet coefficients. In such a case, it becomes essential to further process the wavelet coefficients to obtain informative features like singularities (Kulkarni et al., 2001) or local Hölder exponents (Jade et al., 2006). Moreover, recurrence analysis facilitates the qualitative identification of the state of the multiphase system in form of recurrence plots (RPs), thereby, possibly exploring the applicability of the RPs in qualitative identification of regime of operation and fault diagnosis for bubble column reactors. Thus, for the present study, it was thought desirable to explore the applicability of recurrence analysis method for the first time in design of a multiphase system.

Recent applications of RQA include examples in the field of bioinformatics (Zbilut et al., 2002), financial time-series analysis (Jorge, 2004) and for online damage detection within the system (Nichols et al., 2006). This technique is derived from non-linear dynamics (Schuster and Just, 2005; Kang et al., 2000), and is based on a graphical description of system's dynamics dubbed as the recurrence plot (RP). In short, a RP provides a global, qualitative picture of the correlations between the states of a time-series over all available time-scales. Further, it is possible to reveal underlying structures in the time-series data (determinism) using this approach, which is not readily available to many other approaches, such as methods involving linear transformations of the data (e.g. the Fourier transform). The quantification analysis of the recurrence plots involves estimation of a set of parameters (recurrence parameters) that describe the structures in the plots such as single dots and diagonal, vertical and horizontal lines.

LDA actually measures the instantaneous liquid-phase velocities (Buchhave et al., 1979; Joshi et al., 1996; Kulkarni et al., 2001; Scott, 1974). Bubbles pass through the measurement volume and create a corresponding time-gap (noted hereafter as arrival time-gap) that can be easily identified from the markings on the time-series. Fig. 1 shows a typical LDA signal acquired for one of the positions in bubble column reactor. It is known that while a bubble ascends in the vertical direction, it carries a liquid envelope associated with it. Therefore, the instantaneous liquid velocity associated with a bubble can be considered as the gas-phase velocity. In this way depending on the size and the rise velocity of the ascending bubble, corresponding arrival gap and the velocity amplitude is obtained along the time as the LDA measurements. The main focus of our application is in quantifying the dynamically recurring patterns/states within the local instantaneous velocity–time data for a two-phase bubbly flow system. These recurring patterns as a result of the passage of bubbles and liquid eddies of different sizes through the point of measurement largely depend upon the type of sparger and show variation over the column cross-section. The recurring states are thus related to the local hydrodynamic properties of the system viz. gas hold-up and bubble size. The relation between the recurring dynamical states from LDA time-series using RQA technique and the local hydrodynamic properties is expected to possess a greater sensitivity to changing dynamics than to the linear approaches such as frequencies. In this work, support vector regression (SVR) [a well-known machine learning algorithm (Vapnik et al., 1996; Gunn, 1998; Smola and Scholkopf, 1998)], has been used to relate recurrence parameters to gas hold-up values. Recent application of SVR in design of multiphase reactors can be found in Jade et al. (2006) and Gandhi et al. (2007a,b).

This entire modeling approach is detailed in the form of an algorithm as shown in Fig. 2. The manuscript is organized as follows: The concept and theory of RQA and SVR are discussed in Sections 2 and 3, respectively, while in Section 4 we briefly discuss the experiments. The characteristic variation of the statistical parameters for different data sets and their relation with the local gas hold-up are discussed in Section 5. We also analyze the results obtained under various conditions and discuss possible applications.

2. Recurrence quantification analysis (RQA)

2.1. Recurrence plots

Recurrence is a fundamental property of dissipative dynamical systems (Schuster and Just, 2005). Small disturbances in parameters or operating conditions in such a system can cause exponential

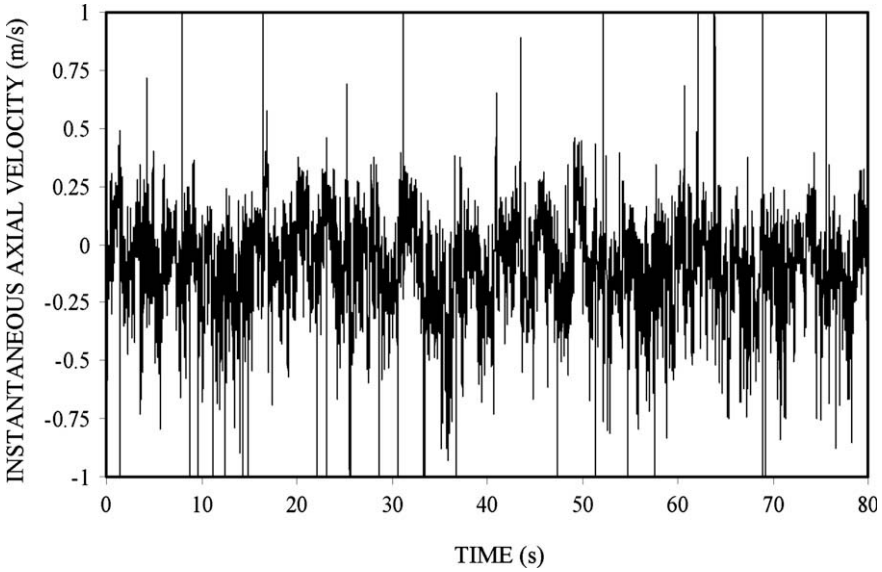

Fig. 1. LDA series: bubble passage.

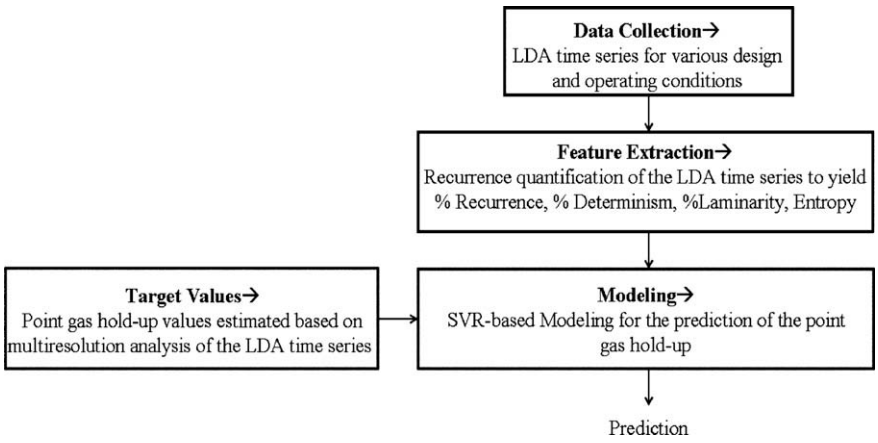

Fig. 2. Flowchart describing modeling steps.

divergence of its state, but the system will come back to a state that is arbitrarily close to a former state and pass through a similar evolution. Ekmann et al. (1987) introduced the concept of *recurrence plot* (*RP*), as a graphical tool that can visualize such recurrent behaviour in a phase-space of a dynamical system. A phase-space is usually a high dimensional space and can only be visualized by projection onto a smaller two- or three-dimensional sub-spaces. RPs enable us to investigate the *m*-dimensional phase-space trajectory through a two-dimensional representation of its recurrences.

Mathematically, given a scalar (one-dimensional) time-series $x(i) = 1,2,3,\ldots N$ an embedding procedure will form a vector, X_i with m the embedding dimension and τ the time lag. RPs are symmetrical array of these vectors placed at (i,j). Whenever a point X_i on the trajectory is close to another point X_j, the closeness between X_i and X_j is expressed by calculating the Euclidian distance between these two normed vectors, $\|X_i\text{-}X_j\| \leqslant r$ where r is a fixed radius. With the aid of the analysis being carried by Heaviside function, Θ (Kang et al., 2000), if the distance falls within this radius, the two vectors are considered to be recurrent and graphically indicated by a white region. Thus, the distance matrices convey all of the relevant information necessary for the global reconstruction of a given system. Such an RP can be mathematically expressed as

$$R_{i,j} = \Theta(r - \|X_i - X_j\|), \quad X_i \in R^m, \quad i,j = 1,\ldots S \tag{1}$$

Detailed mathematical explanation on the same can be found in Marwan (2003) and Webber and Zbilut (2005).

2.2. Determining parameters for RQA

The graphical representation of RPs may be difficult to evaluate, since they are considered as qualitative tools to detect hidden rhythms graphically. However, the RPs can be made quantitative (Zbilut et al., 2004; Webber and Zbilut, 2005) by defining specific rules to automatically extract certain recurrence features. The closer inspection of the RPs reveals small-scale structures (the texture), which are *single dots*, *diagonal lines* as well as *vertical* and *horizontal lines*. These structures are taken into account and quantified by the descriptors used in RQA. These descriptors include: *%recurrence*,*%determinism*, *entropy* and *% laminarity*.

In particular: *Single, isolated recurrence points* can occur if states are rare and if they do not persist or fluctuate heavily. These dots are counted in the quantitative descriptor *%recurrence* (%REC) defined as the number of recurrent points per total triangular area, excluding the central diagonal (which represents the distance between each embedded vector and itself known as recurrence matrix, $R_{i,j}$) and given as,

$$\%REC = \frac{1}{w^2}\sum_{i,j=1}^{w} R_{i,j} \tag{2}$$

where w is the length of the time-series under analysis. Embedded processes that are periodic have higher percent recurrence values than processes that exhibit aperiodic dynamics. It can range from 0% (no recurrent points) to 100% (all points recurrent).

The second recurrence descriptor is *%determinism* (%DET) and measures the proportion of recurrent points forming diagonal line structures. Denoting N_l the number of lines (diagonal) of length l, percent determinism is given by,

$$\%DET = \sum_{l=l_{\min}}^{w} lN_l \Big/ \sum_{i,j}^{w} R_{i,j} \tag{3}$$

Diagonal line segments must have a minimum length, $l_{\min}$ (usually $l_{\min} = 2$) defined by the line parameter. The diagonal length measures how long the lines will be close to each other and can be interpreted as the mean prediction time. Periodic signals (e.g. sine waves) will give very long diagonal lines, whereas chaotic signals (e.g. Hénon attractor) will give very short diagonal lines, and stochastic signals (e.g. random numbers) will give no diagonal lines at all (unless parameter *radius* is set too high).

The third recurrence descriptor is *entropy* (ENT), which is the Shannon information entropy of all diagonal line lengths distributed over integer bins in a histogram. ENT is a measure of signal complexity and is calibrated in units of bits/bin. Individual histogram bin probabilities ($P(l)$) are computed for each non-zero bin and then summed according to Shannon's equation.

$$Entropy = -\sum_{l=l_{\min}}^{w} P(l)\log_2 P(l) \tag{4}$$

As the logarithms are to the base 2, the entropy can be interpreted as number of bits. For simple periodic systems in which all diagonal lines are of equal length, the entropy would be expected to be 0.0 bits/bin (narrow diversity in diagonal line lengths) but relatively high within chaotic windows (wide diversity in diagonal line lengths).

The fourth recurrence descriptor is *% laminarity* (%LAM). A *vertical/horizontal line* marks a length in which a state does not change or changes very slowly (trapped state). These are called laminar re-

gions and are counted in the descriptor laminarity (%LAM). It is analogous to %DET except that it measures the percentage of recurrent points comprising vertical line structures rather than diagonal line structures. Thus, it is the ratio of the recurrence points forming the vertical structures and the entire set of recurrence points. Denoting N_v the number of lines (vertical) of length v, percent laminarity is given by,

$$\%LAM = \sum_{v=v_{\min}}^{w} vNv \Big/ \sum_{i,j}^{w} R_{i,j} \tag{5}$$

However, an appropriate estimation of the aforementioned RQA parameters depends on the phase-space plot, which in turn is constructed based on an appropriate choice of embedding dimension (m), time delay (τ) and *radius* (r).

2.3. Choice of time delay (τ)

An attractor/phase-space represents the time evolution of a hydrodynamical system. Choice of the time delay is crucial, since time delay cannot be too small so that axes are closely related while on the other hand it cannot be too large to avoid the loss of information between axes. In this study, initially the delay time was decided based on the criteria of the first local minimum in mutual information function, however, this approach resulted in wide variation in the values of the time delay and so was with the final RQA parameters and thereby, establishing SVR-based regression function with poor prediction accuracy. Thus, in order to avoid such discrepancy, it was thought desirable to choose the delay time of 1 based on the Takens theorem (Takens, 1981). Since the LDA based velocity–time-series was acquired at 100 Hz, the time delay of 1 in that case stands out to, 1/100 = 0.01 s. With this every consecutive point of the time-series constitutes the delayed vector.

2.4. Choice of embedding dimension (m)

Even after a suitable delay time has been found, it should be taken into account to ensure that the attractor is fully unfolded in the state space with no crossing of orbits/trajectories of the attractor. If m is selected too small, the delayed phase-space cannot completely unfold the attractor such that false nearest neighbours will occur. By sequential increase of the embedding dimension and computation of the corresponding percentage of false neighbors, the minimal embedding dimension can be easily obtained.

2.5. Choice of radius (r)

In effect, the radius parameter implements a cut-off limit (Heaviside function) that transforms the distance matrix (Euclidian distance) into the recurrence matrix (RM). Fig. 3, a "shotgun plot", provides a conceptual framework for understanding why an increasing RADIUS captures more and more recurrent points in phase-space. It represents a hypothetical system in m-dimensional phase-space with a display of points (vector points) surrounding a single reference point (white dot). The points falling within the smallest circle (*radius* = 1 distance units) are the nearest neighbors of the reference point. All such points are recurrent with the reference point. The second concentric circle (*radius* = 2 distance units) includes a few more neighbors, increasing the number of recurrences from 5 to 9. Increasing the radius further (*radius* = 3 or 4 distance units) becomes too inclusive, capturing an additional 15 or 40 distant points as nearest neighbors when, in fact, they are not. Thus, it is desirable to choose the smallest possible radius and thus, based on the suggestions from the literature (Zbilut and Webber, 1992) this threshold should be a few percent of the maximum phase-space diameter and should not exceed 10% of the mean or the maximum phase-space diameter.

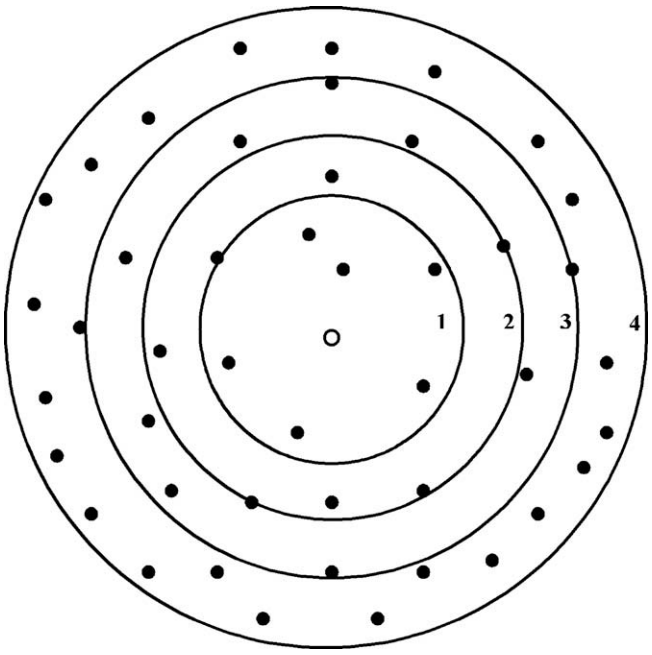

Fig. 3. Two-dimensional representation of a hypothetical system in m-dimensional phase-space with a display of points (closed dots) surrounding a single reference point (white dot). (1) *radius* = 1, (2) *radius* = 2, (3) *radius* = 3, (4) *radius* = 4.

3. SVR-based modeling

3.1. Mathematical modeling

The support vector regression (SVR) is an adaptation of a recently introduced statistical/machine learning theory known as, *support vector machines* (Vapnik et al., 1996). The objective over here is to build a ε-SVR model (Vapnik et al., 1996) to fit a regression function, $y = f(x)$, such that it accurately predicts the outputs $\{y_i\}$ corresponding to a new set of input examples, $\{x_i\}$. In ε-SVR model, ε represents (loss function) the radius of the tube located around the regression function, $f(x)$ (Fig. 4) and the region enclosed

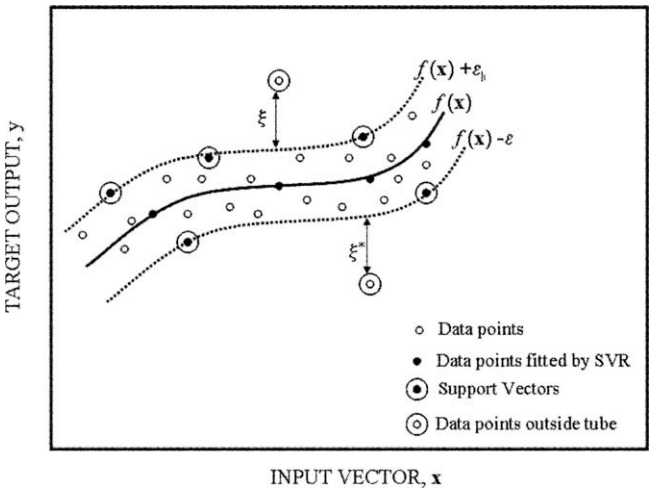

Fig. 4. A schematic illustration of SVR using ε-sensitive loss function by Nandi et al. (2004).

by the tube is known as 'ε- insensitive' zone (Gunn, 1998). The loss function assumes a zero value in this zone and as a result it does not penalize the prediction errors with magnitudes smaller than ε. To fulfill the stated goal, SVR considers the following linear estimation function in the high dimensional feature space (Smola and Scholkopf, 1998),

$$f(x,w) = (w \bullet \phi(x) + b) \tag{6}$$

where, $\phi(x)$ = function termed *feature* and ($w \bullet \phi(x)$) the dot product in the feature space, F, such that $\phi(x) \to F$, and $w \in F$. Thus after algebraic transformation the objective function Eq. (6), gets converted to convex optimization problem (Gunn, 1998; Smola and Scholkopf, 1998; Vapnik et al., 1996). The primal form of the optimization problem is given as,

$$\text{Maximize } (L(\alpha_{i,j}^{(*)}) = \sum_{i=1}^{N} y_i(\alpha_i - \alpha_i^*) - \varepsilon \sum_{i=1}^{N}(\alpha_i + \alpha_i^*)) - \frac{1}{2}\sum_{i=1}^{N}\sum_{j=1}^{N}(\alpha_i - \alpha_i^*)(\alpha_j - \alpha_j^*)(\phi(x_i) \bullet \phi(x_j)) \tag{7}$$

Subject to constraints $C \geqslant \alpha_i, \alpha_i^* \geqslant 0$ and $\sum_{i=1}^{N}(\alpha_i - \alpha_i^*)y_i = 0$
where, C = cost function employed to obtain a trade-off between the *flatness* of the regression function and the amount to which deviations larger than ε can be tolerated. Solving this problem Eq. (7) by convex quadratic programming (QP) gives the value of the coefficients α and α_i^*. Owing to the specific character of the above-described quadratic programming problem, only some of the coefficients, $(\alpha - \alpha_i^*)$, are non-zero and the corresponding input vectors, x_i, are called support vectors (SVs). These SVs are known to be as the most informative data points that compress the information content of the training set, thereby representing the entire SVR function. The coefficients α and α_i^* have an intuitive interpretation as forces pushing and pulling the regression estimate $f(x)$ towards the measurements, y_i. It can be seen in Fig. 4, that SVs are depicted as points lying on the surface of the tube and the regression function can be fully characterized by these support vectors. Owing to this characteristic the final regression model can be defined with the help of relatively small numbers of input vectors. These SVs, x_i and the corresponding non-zero Lagrange multipliers α and α_i^* give the value of weight vector, w followed by the expanded form of the SVR,

$$w = \sum_{i=1}^{N}(\alpha_i - \alpha_i^*)\phi(x_i) \tag{8}$$

$$f(x, \alpha_i, \alpha_i^*) = \sum_{i=1}^{Nsv}(\alpha_i - \alpha_i^*)(\phi(x_i) \bullet \phi(x_j)) + b \tag{9}$$

However, for the aforementioned optimization problem Eq. (7) with the increase in the input dimensions the dimensions in the high dimensional feature space further increases by many folds and thus becomes a computationally intractable problem. Such a problem can be overcome by defining appropriate kernel functions in place of the dot product of the input vectors in high dimensional feature space.

$$K(x_i, x_j) = (\phi(x_i) \bullet \phi(x_j)) \tag{10}$$

The advantage of a kernel function is that the dot product in the feature space can now be computed without actually mapping the input vectors, x_i into high dimensional feature space. Thus, when using a kernel function all the necessary computations can be performed implicitly in the input space instead of in the feature space. Thus, the basic SVR formulation takes following the form,

$$f(x, \alpha_i, \alpha_i^*) = \sum_{i=1}^{Nsv}(\alpha_i - \alpha_i^*)K(x_i, x_j) + b \tag{11}$$

Table 1
Design and operating conditions of LDA measurement

Sr. No.	Sparger type	Superficial gas velocity (m/s)	r/R (−)	z/R (−)	Number of data points
1	SPS	0.02	0–0.933	0.4 & 5.2	30
2	MPS	0.02	0–0.860	0.4 & 2.8	23

Also the bias parameter, b, can be computed by applying Karush–Kuhn–Tucker (KKT) conditions, which states that at the optimal solution the product between dual variables and constraints has to vanish. Thus giving,

$$b = \{y_i - (\alpha_i - \alpha_i^*)K(x, x_i) - \varepsilon\} \quad \text{for } \alpha_i \in \langle 0, C\rangle$$
$$b = \{y_i - (\alpha_i - \alpha_i^*)K(x, x_i) + \varepsilon\} \quad \text{for } \alpha_i^* \in \langle 0, C\rangle \tag{12}$$

where x_i and y_i, respectively, denote the ith SV and the corresponding target output. There exist several choices of kernel function K like linear, polynomial and Gaussian radial basis function. The most commonly used kernel function is the Gaussian radial basis function (RBF) (Gunn, 1998; Vapnik et al., 1996).

3.2. Procedure for estimating regression function

In the present study, a SVR-implementation known as "ε-SVR" in the LIBSVM software library (Chang and Lin, 2001) has been used to develop the SVR-based model for overall gas hold-up. Detailed procedure for estimating regression function can be obtained from Gandhi et al. (2007a,b).

4. Experimental work

Experiments were carried out in a cylindrical Plexiglass bubble column of 150 mm internal diameter for the gas–liquid system with LDA measurements taken for the axial velocity component. This column was enclosed in another column of square cross-section and the space between the two was filled with water to minimize refraction effects. An oil free diaphragm type compressor was used to sparge air through the spargers. The clear liquid height of

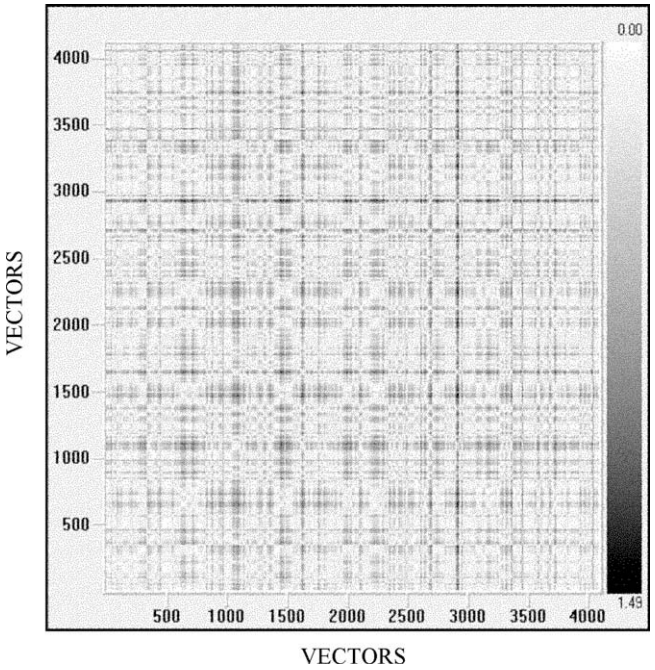

Fig. 5. Recurrence Plot (RP) of LDA time-series for MPS (A) $r/R = 0$, $Z/R = 2.8$, (B) $r/R = 0.86$, $Z/D = 1.4$.

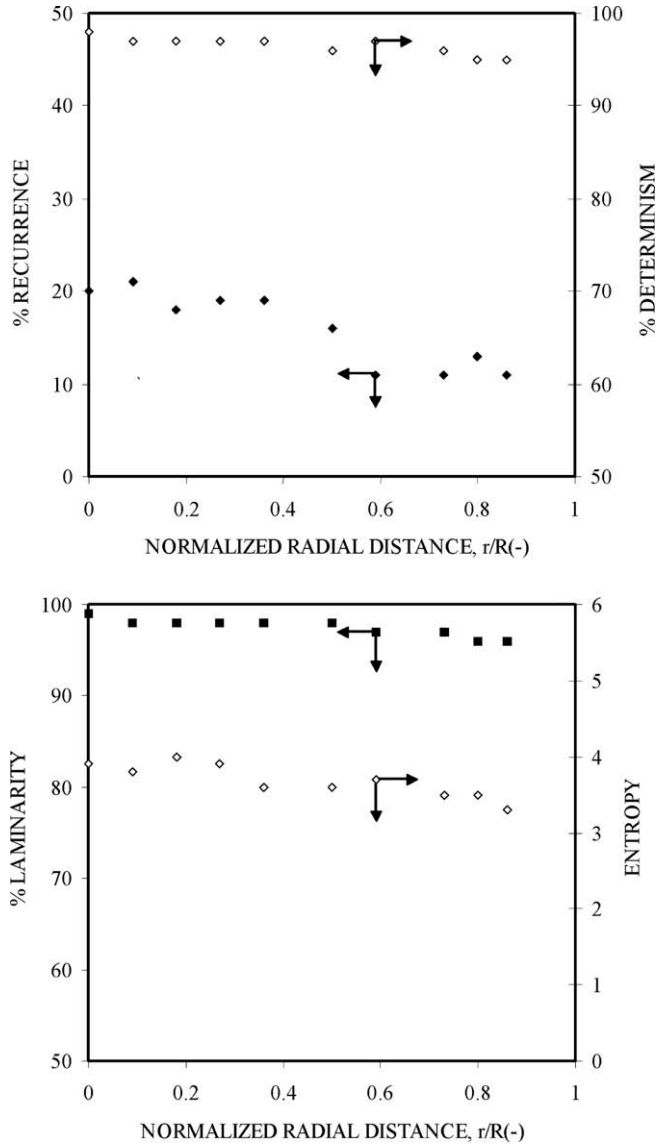

Fig. 6. Variation of recurrence parameters as a function of normalized radial distance of the column for MPS at $Z/D = 1.4$.

tap water in the cylindrical column was 900 mm. Details about the LDA measurement locations are mentioned in the Table 1. The LDA set-up comprised of a Dantec 55X modular series along with electronic instrumentation and a personal computer (80586). A 5 W Argon–ion laser was used as a source. The LDA measurements were carried out at several levels from the sparger. The purpose was to understand the development of gas hold-up flow profile in the column and hence it was necessary to acquire the data at different axial levels, where, $z/D = 0$ is the sparger. The different values of z/D chosen in these experiments were mainly because of the height above the sparger where the measurements could be done without any obstacles. This issue was important as the measurements were done in forward scatter mode. More details about the LDA measurements for the system can be found in Kulkarni et al. (2001).

5. Results and discussion

5.1. RQA analysis of LDA time-series

RPs were constructed from the individual LDA time-series [4096 data points] for the defined set of operating and design conditions (Table 1). A time delay (τ) of 1 was chosen based on Takens theorem whereas the minimal embedding dimensions (m) were estimated based on percentage of false nearest neighbors and they were seen to yield values of 4 and 2 for Multipoint point sparger and Single point sparger respectively. Threshold was not allowed to exceed beyond 10% of the maximum phase-space diameter and thereby setting a uniform value of, $r = 0.1$. Fig. 5 shows a typical RP constructed from the LDA time series for Multipoint point sparger. This qualitative pattern of RP is further quantified by RQA in terms of % REC, % DET, %LAM and Entropy. Figs. 6 and 7 show the plots of the values for each of these quantified parameters as a function of normalized radial distance of the bubble column, for Single point sparger and Multipoint point sparger respectively. These quantified values are based on the LDA time-series acquired in the bulk region of the column ($Z/D = 1.4$ and 2.6 for Multipoint point sparger and Single point sparger, respectively). Comparing the recurrence quantified values for both the spargers along the column radius; it is observed that for Single point sparger, relatively higher recurrence is observed in the centre region of the column, than that for Multipoint point sparger. Such behaviour is along the lines of the gas hold-up profiles for both the

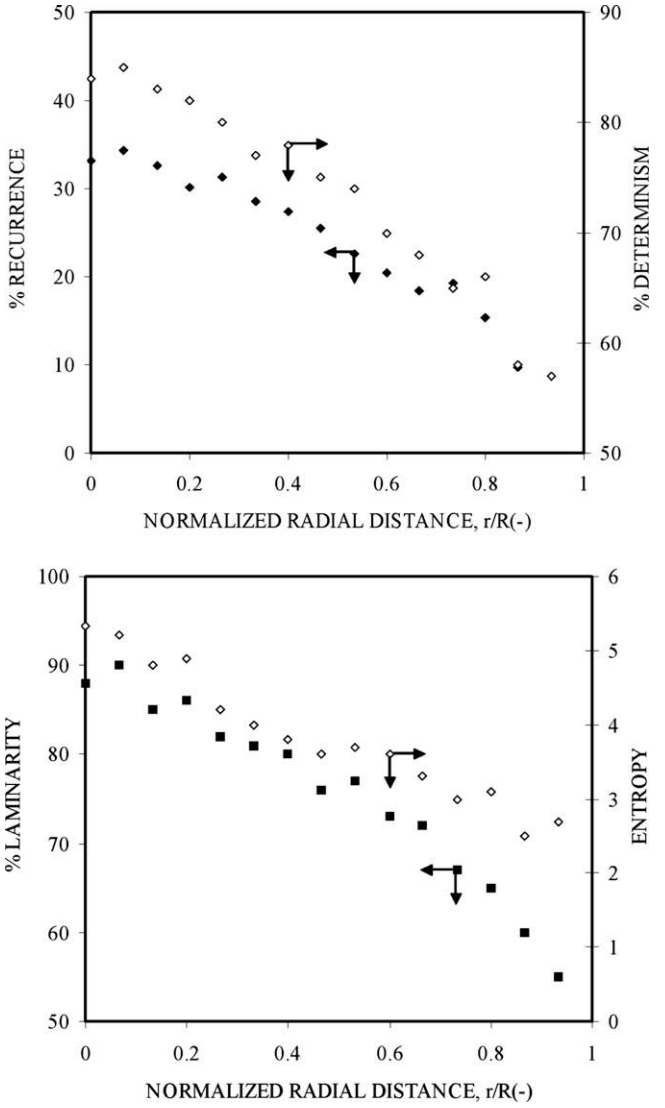

Fig. 7. Variation of recurrence parameters as a function of normalized radial distance of the column for SPS at $Z/D = 2.6$.

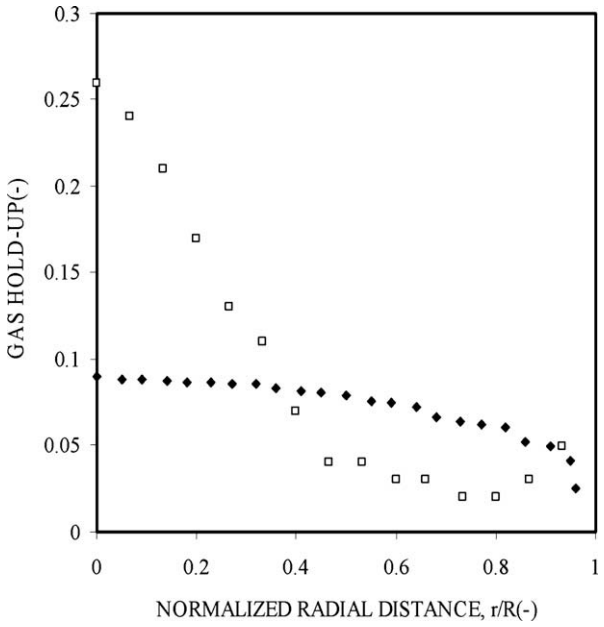

Fig. 8. Radial variation of fractional gas hold-up for ♦ MPS (Z/D = 1.4), SPS (Z/D = 2.6).

spargers. For Single point sparger it is known to have a steep gas hold-up profile, while that for Multipoint point sparger has a relatively flat profile for the bulk region of the bubble column as shown in Fig. 8.

5.2. Recurrence quantified parameters based SVR modeling

SVR model for multi point sparger was developed for predicting the local point gas hold-up. The model was established based on 53 data points and 8 features (V_G, r/R, z/D, sparger distribution coefficient, %REC, %DET, %LAM, ENT) as input vectors. As mentioned earlier, in the present study, an SVR-implementation known as "ε-SVR" in the LIBSVM software library was used to develop the SVR-based model. RBF kernel resulted in the least MSE values and maximum squared CC values for the model. To avoid the possibility of arbitrary predictions arising out of insufficient training data, a method known as "*leave-one-out*" was used to select an optimal model. An average of the MSEs corresponding to the left-out subsets, known as "loo error (MSE_{loo})" gives an estimate of the model performance if a large-sized data set was available for building the model. After evaluation of the model for a wide range of model parameters (grid search methodology), the optimal values of the three SVR-specific parameters namely, width of RBF kernel (σ), cost coefficient (C) and loss function parameter (ε_{loss}), are listed in Table 2. The values of CC_{loo} along with the corresponding MSE_{loo} values for the model are listed in Table 3. Selection of the optimal model parameters automatically decides the optimal number of support vectors (31), which play a vital role in the performance of the SVR-based model.

As a part of this work, we also checked as to how well the entire approach predicts the point gas hold-up values for the conditions which were not included in the databank for training the model i.e., test dataset. In all three LDA time-series were used as the test dataset. These LDA time-series were acquired for Multipoint point sparger at the superficial gas velocity of 0.012 m/s, at axial location of Z/D = 1.4 and at three different radial positions of r/R = 0.0, 0.027 and 0.9 respectively. The experimentally measured fraction gas hold-up values at these three locations are 0.072, 0.071 and 0.042, while the predictions based on our model yields 0.075, 0.074 and 0.04, respectively for the same locations. The difference between the experimental and the model predictions is less than 5% and hence justify the use of a trained model based on RQA and SVM for the estimation of the local fractional gas hold-up from such an analysis.

Appendix B represents the detailed pictorial algorithm for the aforementioned modeling approach.

Table 2
Parameter selection for SVR-based model for multi point sparger

Model	C	$\gamma = \frac{1}{2\sigma^2}$	ε_{loss}	Number of support vectors	Number of training data points
Point gas hold-up	2	1.21	0.0045	31	53

Table 3
Performance indicators for the SVR-based model for point gas hold-up

Correlation coefficient (CC)	Mean square error (MSE)
CC_{loo} = 0.872	MSE_{loo} = 0.00036
CC_{train_model} = 0.981	MSE_{train_model} = 0.000077
CC_{test_model} = 0.960	MSE_{test_model} = 0.000068

6. Conclusion

This work demonstrates the application of recurrence plots and recurrence quantification analysis (RQA) for detecting recurring dynamical states, within LDA time-series for bubble column reactors. The point gas hold-up value, which is a function of the bubble characteristic at the point of measurement, is implicitly related to the recurrence quantified values.

SVR, a robust machine learning based non-linear modeling paradigm at various design conditions possessing several desirable features was used to establish a non-linear relation between point gas hold-up and the so obtained recurrence quantified parameters. The proposed models exhibit reasonably high prediction accuracy and can be used for real-time prediction of point gas hold-up values. Such SVR-based models for bubble column can be potentially useful on commercial scale for online monitoring and control of point gas hold-up. The applicability of this tool for the data for different measurement techniques can be easily generalized.

Acknowledgements

ABG thanks Council of Scientific and Industrial Research (CSIR), the Govt. of India, New Delhi, for a Senior Research Fellowship (SRF). VKJ wishes to acknowledge the support received from NCL in the form of an in house project Grant No.: MLP 011726.

Appendix 1. Detailed mathematical and graphical presentation of the procedure for the construction of the recurrence plot and estimation of recurrence parameters

(a) Explicit example of how recurrence plots are constructed is detailed below for a contrived time-series vector (TS) with 29 elements.*TS* = [3.7, 9.2, 2.1, −5.4, 0.0, −10.9, 9.2, 3.1, 1.7, 1.8, −0.3, −4.9, 2.7, 3.5, 7.5, −9.9, −9.9, −4.7, 1.3, 2.7, 7.6, 3.9, 7.3, 8.0, 0.3, −1.9, 5.1, 8.8, 8.2]

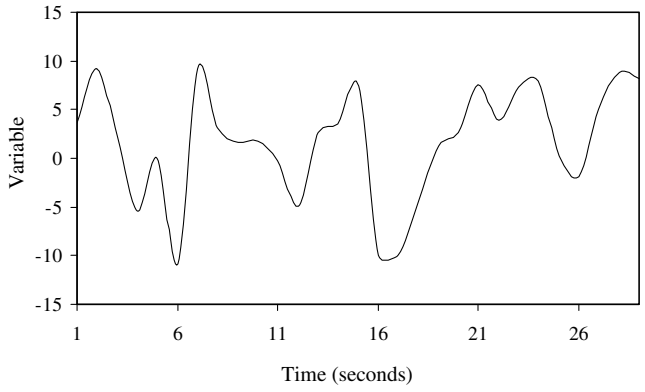

(b) For time delay (τ) = 8, and embedding dimension (m) = 4, the following 5 time-delayed vectors are constructed in specified units (V).

$$V1 = [+3.7, +1.7, -9.9, +0.3]$$

$$V2 = [+9.2, +1.8, -4.7, -1.9]$$

$$V3 = [+2.1, -0.3, +1.3, +5.1]$$

$$V4 = [-5.4, -4.9, +2.7, +8.8]$$

$$V5 = [+0.0, +2.7, +7.6, +8.2]$$

(c) Next, the Euclidean distance in the distance matrix (DM) between vectors V4 and V5 is calculated as follows, DM (4,5).

$$\begin{aligned}\mathrm{DM(Euclid)} &= \mathrm{SQRT(SQR}(-5.4-0.0)+\mathrm{SQR}(-4.9-2.7)\\ &\quad+\mathrm{SQR}(2.7-7.6)+\mathrm{SQR}(8.8-8.2))\\ &= 10.549\end{aligned}$$

This procedure is repeated for each cell, giving the following results for DM (i,j). Here only the distances in the upper triangle are shown since the lower half is perfectly symmetrical. Note that the central diagonal is designated by 0.000 distances (vector identity matches).

DM(Euclid norm) =

$[1, 5] = 19.579; [2, 5] = 18.405; [3, 5] = 7.919; [4,5] = 10.549; [5, 5] = 0.000$

$[1, 4] = 18.904; [2, 4] = 20.671; [3, 4] = 9.647; [4, 4] = 0.0000; [5, 4] = 10.549$

$[1, 3] = 12.452; [2, 3] = 11.825; [3, 3] = 0.000; [4, 3] = 9.647; [5, 3] = 7.919$

$[1, 2] = 7.883; [2, 2] = 0.0000; [3, 2] = 11.82; [4, 2] = 20.671; [5, 2] = 18.405$

$[1, 1] = 0.000; [2, 1] = 7.883; [3, 1] = 12.4; [4, 1] = 18.90; [5, 1] = 19.579$

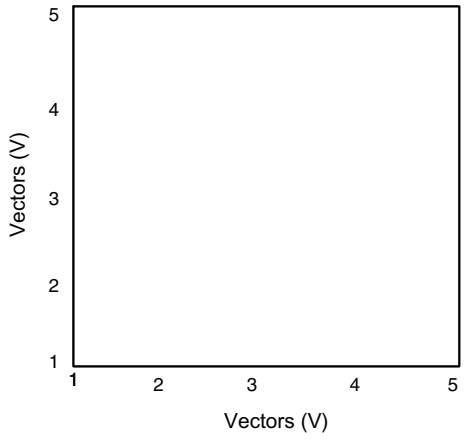

(d) Recurrence matrices RM [i,j] and thereafter the recurrence plots, RPs are derived from distance matrices by setting a radius (r) threshold. As shown below, the Heaviside function assigns values of 0 or 1 to array elements. Only those distances in RM [i,j] equal to or less than the radius (r) are defined as recurrent points at coordinates i, j.

RM(Euclid norm with RADIUS of 8.0) =

$[1, 5] = 0; [2, 5] = 0; [3, 5] = 1; [4, 5] = 0; [5, 5] = 1$

$[1, 4] = 0; [2, 4] = 0; [3, 4] = 0; [4, 4] = 1; [5, 4] = 0$

$[1, 3] = 0; [2, 3] = 0; [3, 3] = 1; [4, 3] = 0; [5, 3] = 1$

$[1, 2] = 1; [2, 2] = 1; [3, 2] = 0; [4, 2] = 0; [5, 2] = 0$

$[1, 1] = 1; [2, 1] = 1; [3, 1] = 0; [4, 1] = 0; [5, 1] = 0$

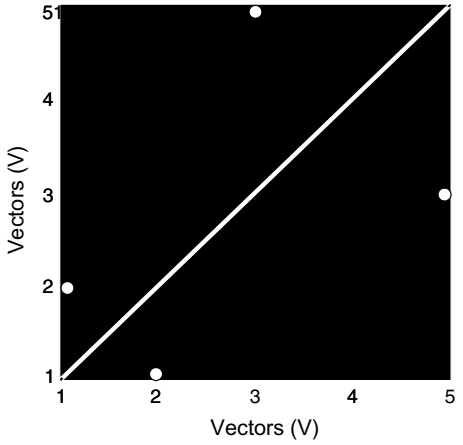

Thus, based on the so obtained RM [i,j], the single dot, diagonal and vertical horizontal lines structure, also known as recurrence plot (RP) is generated. We would like to indicate that '0' are indicated by black color and '1' to be indicated by white color in the RPs. Thus, the white colored single dot, diagonal and vertical horizontal lines structure show the extent of recurrence within the RPs.

A typical, RP is shown below having, (1) A line segment composed of four recurrent points, (2) several recurrent points not the part of the line segment, (3) A line segment composed of four points representing laminarity, (4) the identity line,

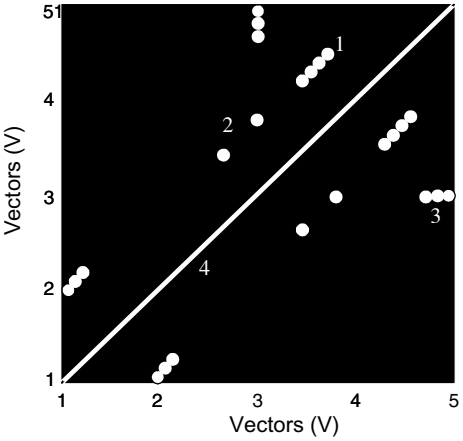

(e) RQA looks for patterns among these recurrent points of RM [i,j], to define the RQA variables: *% recurrence*, *% determinism*, *entropy* and *% laminarity*. Further details about the calculation of these parameters are given in Section 2.2, '*Determining parameters for RQA*' of the paper.

Appendix 2. Detailed algorithm representing the entire modeling approach

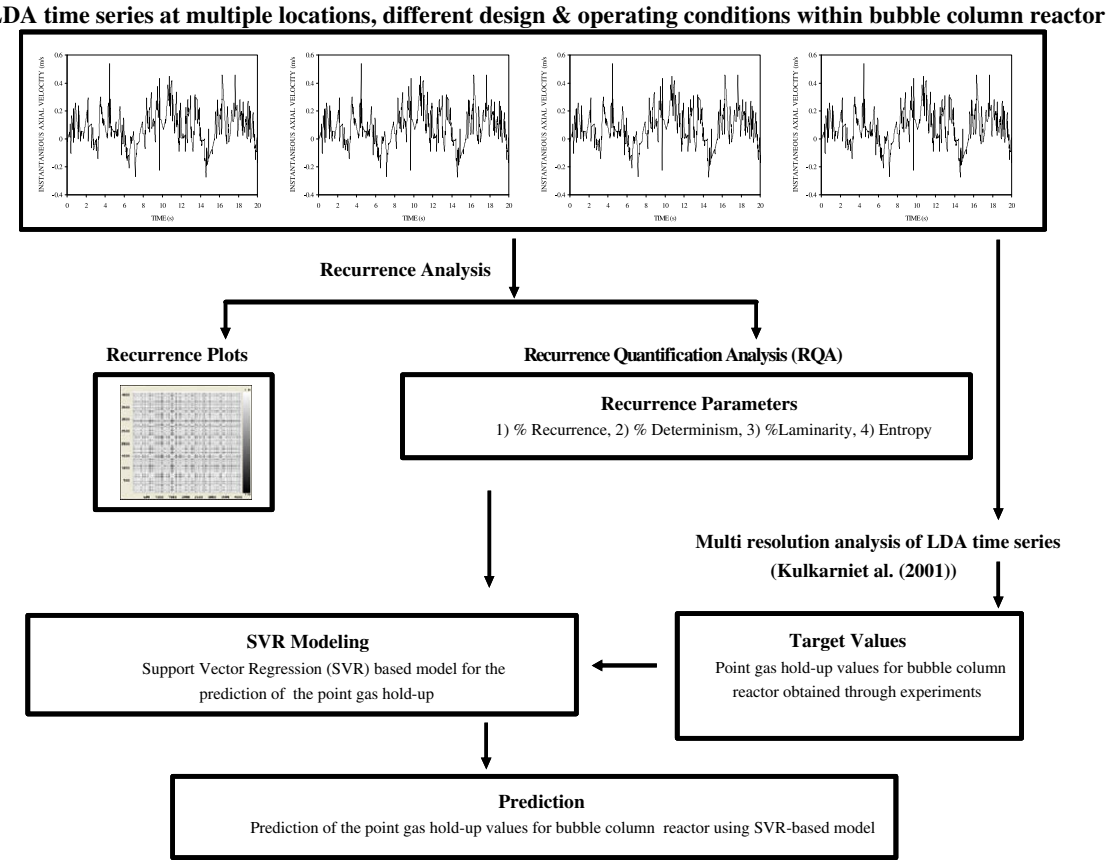

References

Buchhave, P., George Jr., W.K., Lumley, J.L., 1979. The measurement of turbulence with the laser Doppler anemometer. Annu. Rev. Fluid Mech. 11, 442–503.

Castellini, H., Romanelli, L., 2004. Applications of recurrence quantified analysis to study the dynamics of chaotic chemical reaction. Physica A 342, 301–307.

Chang, C.-C., Lin, C.-J., LIBSVM: A library for support vector machines. Software Available from: <http://www.csie.ntu.edu.tw/~cjlin/libsvm.2001>.

Ekmann, J.P., Kamphorst, S.O., Ruelle, D., 1987. Recurrence plots of dynamical systems. EuroPhys. Lett. 4, 324–327.

Gandhi, A.B., Joshi, J.B., Jayaraman, V.K., Kulkarni, B.D., 2007a. Data-driven dynamic modeling and control of a surface aeration system. Ind. Eng. Chem. Res. 46 (25), 8607–8613.

Gandhi, A.B., Joshi, J.B., Jayaraman, V.K., Kulkarni, B.D., 2007b. Support vector regression (SVR)-based correlation for prediction of overall gas hold-up in bubble column reactors for various gas–liquid systems. Chem. Eng. Sci. 62, 7078–7089.

Gunn, S.R., 1998. Support vector machines for classification and regression. Technical Report, Department of Electronics and Computer Science. University of Southampton. Available from: <http://trevinca.ei.uvigo.es/~cernadas/tc03/mc/SVM.pdf>.

Jade, A.M., Jayaraman, V.K., Kulkarni, B.D., Khopkar, A.R., Ranade, V.V., Sharma, A.A., 2006. A novel local singularity distribution based method for flow regime identification: gas–liquid stirred vessel with Rushton turbine. Chem. Eng. Sci. 61, 688–697.

Jorge, B.F., 2004. Testing for non-linearity in an artificial financial market: a recurrence quantification approach. J. Econ. Behav. Organ. 54, 483–494.

Joshi, J.B., Elias, C.B., Patole, M.S., 1996. Role of hydrodynamic shear in the cultivation of animal, plant and microbial cells. Chem. Eng. J. Biochem. Eng. J. 62, 121–141.

Kang, Y., Cho, Y.J., Woo, K.J., Kim, K.I., Kim, S.D., 2000. Bubble properties pressure fluctuations pressurized bubble columns. Chem. Eng. Sci. 55, 411–419.

Kulkarni, A.A., Joshi, J.B., Ravi Kumar, V., Kulkarni, B.D., 2001. Application of multiresolution analysis for simultaneous measurement of gas and liquid velocities and fractional gas hold-up in bubble column using LDA. Chem. Eng. Sci. 56, 5037–5048.

Letzel, H.M., Schouten, J.C., Krishna, R., Van den Bleek, C.M., 1997. Characterization of regimes and regime transitions in bubble columns by chaos analysis of pressure signals. Chem. Eng. Sci. 52 (24), 4447–4459 .

Marwan, N., 2003. Encounters with neighbours: current developments of concepts based on recurrence plots and their applications. Ph.D. Thesis, University of Potsdam. 1-79. Available from: <http://www.recurrence-plot.tk/thesis.php>.

Nandi, S., Badhe, Y., Lonari, J., Sridevi, U., Rao, B.S., Tambe, S.S., Kulkarni, B.D., 2004. Hybrid process modeling and optimization strategies integrating neural networks/support vector regression and genetic algorithms: study of benzene isopropylation on Hbeta catalyst. Chem. Eng. J. 97, 115–129.

Nichols, J.M., Trickey, S.T., Seaver, M., 2006. Damage detection using multivariate recurrence quantification analysis. Mech. Syst. Signal Process. 20, 421–437.

Sen, A.K., Longwic, R., Litak, G., GÖrski, K., 2008. Analysis of cycle-to-cycle pressure oscillations in a diesel engine. Mech. Syst. Signal Process. 22, 362–373.

Schuster, H.G., Just, W., 2005. Deterministic Chaos-An Introduction. Wiley-VCH, Weinheim.

Scott, P.F., 1974. Theory and implementation of Laser velocimeter turbulence spectrum measurement. Proceedings 2nd International workshop on laser velocimetry, 47–67.

Smola, A.J., Scholkopf, B., 1998. A tutorial on support vector regression. Neuro-COLT Technical Report NC-TR-98-030, Royal Holloway College, University of London, UK.

Takens, F., 1981. Detecting strange attractors in turbulence. In: Rand, D.A., Young, L.S. (Eds.), Dynamical Systems and Turbulence. Springer, Berlin.

Van den Bleek, C.M., Schouten, J.C., 1993. Deterministic chaos: a new tool in fluidized bed design and operation. Chem. Eng. J. 53, 75–87.

Vapnik, V., Golowich, S., Smola, A.J., 1996. Support vector method for function approximation, regression estimation and signal processing. Advanced Neural Information Processing System 9, 281–287.

Webber Jr, C.L., Zbilut, J.P., 2005. Recurrecne quantification analysis of nonlinear dynamical systems. In: tutorials in contemporary nonlinear methods for the behavioral sciences web book, eds.: M.A. Riley and G.C. Van Orden, National Science Foundation (U.S.).26-94. Available from: <http://www.nsf.gov/sbe/bcs/pac/nmbs/nmbs.jsp>.

Zbilut, J.P., Giuliani, P.S., Manetti, A.C., Colosimo, A., Webber, C.L., 2002. Review of nonlinear analysis of proteins through recurrence quantification. Cell Biochem. Biophys. 36, 67–87.

Zbilut, J.P., Thomasson, N., Webber, C.L., 2004. Recurrence quantification analysis as a tool for nonlinear exploration of nonstationary cardiac signals. Med. Eng. Phys. 24, 53–60.

Zbilut, J.P., Webber, C.L., 1992. Embeddings and delays as derived from quantification of recurrence plots. Phys. Lett. A 171, 199–203.